

## Profile-Based Lifetime Determination Schemes for Mobility Management in HMIPv6\*

SUN OK YANG, SUNGSUK KIM<sup>†</sup> AND CHONG-SUN HWANG

*Department of Computer Science and Engineering*

*Korea University*

*Seoul, 136-701 Korea*

<sup>†</sup>*Department of Electronic Business*

*Seokyeong University*

*Seoul, 136-704 Korea*

In Mobile IP, whether mobile nodes are moving or not, lots of messages have to be exchanged for various purposes. The frequent exchange of messages incurs overhead in several ways, especially in terms of energy use in mobile node. Of course, if fewer messages are delivered, issues related with authorization may become problematic. To deal with this situation properly, we propose new profile-based lifetime determination schemes. Our works are motivated by the observation that some people perform regular movements; thus, the related information can be useful for decreasing the number of messages forwarded. Therefore, each user can maintain a local profile based on movement logs. From the profile, the proper lifetime for a binding update message can be determined, which will also affect authorization for binding between mobile node and correspondent nodes. In extensive experiments, we mainly focused on bandwidth use for binding update messages. From the results, we found that our schemes can achieve considerable performance improvement by reducing the number of binding update messages at a small additional cost for the profile, which is an essential property in mobile computing environments.

**Keywords:** hierarchical MIPv6, binding update, lifetime determination, profile, mobility type

### 1. INTRODUCTION

At the beginning of the twenty-first century, we face very fast development of two communication technologies: mobile networks and the Internet. The paradigm of communication anywhere anytime has also become realistic. Along with these trends, Internet users now seek connection to the Internet while they are on the move. To accommodate the demand for mobility, Mobile IP (MIP) was proposed. Binding update (BU) and request (BR) messages are used to allow mobile nodes (MNs) to move while maintaining reachability and on going connections between them and correspondent nodes (CNs).

In Mobile IPv6 (MIPv6) [1], an MN sends a BU to the home agent (HA) or CNs

---

Received March 19, 2004; revised October 11, 2004; accepted January 26, 2005.

Communicated by David Du.

\* Sun Ok Yang, SungSuk Kim, Chong-Sun Hwang, and SangKeun Lee, "Energy-efficient message management algorithms in HMIPv6," in Proceedings of the International Conference on Computer Science and its Applications 2004 (ICCSA '04), Assisi, Italy, Vol. 8, pp. 281-289, May, 2004 (LNCS).

<sup>†</sup> This research was supported by University IT Research Center Project.

<sup>†</sup> Corresponding author.

once every 1 second to 7 minutes to report its current location. A return routability mechanism [2] is also used to authorize the establishment of binding. In this situation, whether MNs are moving or not, lots of messages will be exchanged repeatedly. Naturally, issues related with the traffic load for HA, energy efficiency in MN and secure wireless communication have to be considered together.

The authors in [3] proposed a secure and lightweight extension of return routability. They incorporate *Lifetime Credit Authorization* into BU. When an MN needs to re-establish binding, it calculates the next *Kcredit* based on the previous *Kcredit* and the latest *Kbm*. Thus, signaling can be reduced, and the MN is required to wake up frequently (i.e., the upper bound of its lifetime is 8 hours). However, the authors assumed that the MN is a stable node, which may become a problem. If some information about each MN's movement pattern is known in advance, this assumption can be removed, and this is a main goal of our research.

An MN gathers movement logs whenever it leaves a subnet and periodically computes profile information. When it moves into any subnet, it first checks whether there is any record of the subnet in the profile; if there is, the current resident time is guessed, and the proper lifetime is calculated by considering the past mobility pattern. The lifetime also affects the return routability mechanism based on the work reported in [3]. Otherwise, a default mechanism in HMIPv6 is used. Our schemes incur extra costs in maintaining a profile on the MN side. But this cost is not significant since low power consumption, high capacity, and cheap storage devices are commonly available. In contrast, an MN can reduce the number of messages and thus utilize less battery power. In addition, the traffic load for HA is also lightened. This can be a very valuable result in mobile computing. To the best of our knowledge, our work is the first attempt to apply profiles in message management. Thus, we compared our schemes with HMIPv6 in experiments.

The rest of the paper is organized as follows. First, related work will be summarized in section 2. In section 3, we will explain our profile-based lifetime determination algorithms and experiment results will be given in section 4. As a conclusion of this paper, section 5 will summarize our schemes and future research.

## 2. RELATED WORK

Profiles have been applied in various areas. First, they are used in PCS to cope with unlimited user mobility. The authors in [4] showed that mobility management occupies a significant fraction of the network traffic and processing load. This trend is expected to also be reflected in wireless networks.

In a profile-based location update strategy [5], the system maintains a sequential list. This strategy is better than the fixed paging area strategy, but the lack of update protocols makes this strategy infeasible. The authors in [6] proposed a location tracking strategy based on the mobile's movement behavior. In [7], the authors in proposed that each terminal use the history to remove loops in the terminal's movement path. The authors in [6, 7], however, only took into account movement behavior, not the resident time per location. In [8], the authors proposed storing each user's profile at his home location register and using each node in the tree to maintain the subprofile. As long as a user moves to a

sibling node listed in the subprofile stored at its parent, no location update message is sent. However, this approach increases the lookup delay and memory requirements on the network side.

The profile-based mobile MPLS approach proposed in [9], on the other hand eliminates the triangle routing in the current mobile MPLS protocol. The authors in [10] employed the profile in the routing strategy in MANET. In [11], the multi-layered mobility anchor point (MAP) and an appropriate MAP selection procedure were proposed to reduce the concentrative load at a specific MAP by using the MN's mobile history. The authors in [12] presented a hierarchical scheme that enables any CN to cache two CoAs based on the use of two lifetimes for route optimization. However, they did not explain how the lifetime value of BU in HMIPv6 could be determined. These approaches to MIP did not focus on eliminating all the signaling that occurs when an MN stays for a long time at the same location. If signaling is reduced, security [13] may become an issue.

To solve the above problem, an enhanced route optimization security mechanism for MIPv6 [14] is proposed here. In this work, cryptographically generated addresses (CGAs) provide a method for binding a public key to an IPv6 address. The maximum allowed lifetime is 24 hours. This requires, however, extra signaling, and some modifications of signaling have to be made. The authors in [3] proposed a mechanism which can reduce the amount of signaling needed for BUs without exposing nodes to significant new vulnerabilities. It does not require any modifications to the actual return routability test or BUs. However, this only works well when the MN stays for a long time at the same location. Therefore, there is necessary to devise a new scheme to overcome these limitations.

### 3. PROFILE-BASED LIFETIME DETERMINATION

In this section, we will describe our schemes. First, we will discuss the credit-based approach [3], since it will be used as a return routability mechanism [1] in our work. Then, a new type of BU message and related algorithms for determining the BU lifetime will be explained in detail.

#### 3.1 Return Routability

MIPv6 allows a node to redirect packets that the CN would otherwise send to one IP address (the home address) and then to a second IP address (CoA). Redirection can be misused by a malicious node if appropriate precautions are not taken. Thus, MIPv6 requires periodic return routability tests and the re-establishment of binding at the CN [1]. Such authorization should be performed every 7 minutes. This can become a burden for MNs that have bindings ready for possible packets but are not currently communicating. This can be problematic for MNs in standby mode.

To solve this problem, the authors in [3] included the *Lifetime Credit Authorization* option in BU and BA, where the content is based on the binding management key (*K<sub>bm</sub>*) [1]. Instead of being subjected to a fixed limit (7 minutes), an MN can continue to use an existing address test longer than the time it has already been reachable at this address. To authorize this, it has to provide a keyed hash using the key *K<sub>credit</sub>*, calculated as follows:

$$Kcredit = \text{hash}(KbmN | \text{hash}(KbmN - 1 | \text{hash}(KbmN - 2 | \dots Kbm1))).$$

Here,  $Kbm1$  through  $KbmN$  are used to calculate the *Binding Authorization Data* option in the BU and all subsequent BUs.  $Kcredit$  is calculated based on the previous  $Kcredit$  and the latest  $Kbm$ . Both the MN and CNs should hold some state in the binding cache entries, related to credit authorization. The following conceptual information must be kept: the total time when there has been a binding for this home address, the current  $Kcredit$  value, and the number of  $Kbm$  values included in the  $Kcredit$  value.

In this way, it can reduce the number of exchanged messages, since the lifetime can be very long (up to 8 hours). However, it is assumed that the MN is a stable mode. To remove this assumption, local profile information containing each user mobility pattern will be used (as explained in the next subsection).

### 3.2 BU Messages

Hierarchical Mobile IPv6 (HMIPv6) [15], which differentiates local mobility from global mobility is appropriate for the Internet. For this purpose, the mobility anchor point (MAP) is introduced, and its localized mobility domain is called the MAP domain (see Fig. 1). Two addresses are used for communication between the MN and CN: one is the regional care-of address (RCoA), which is an address in the MAP's domain, and the other is the on-link care-of address (LCoA), which is the MN's address obtained from a foreign subnet. The MAP intercepts all the packets from the HA or CNs and tunnels them to the MN's LCoA. Thus, the MN does not need to send BUs to HA and CNs when there is intra-domain movement, but BUs have to be delivered periodically to MAP in spite of HMIPv6.

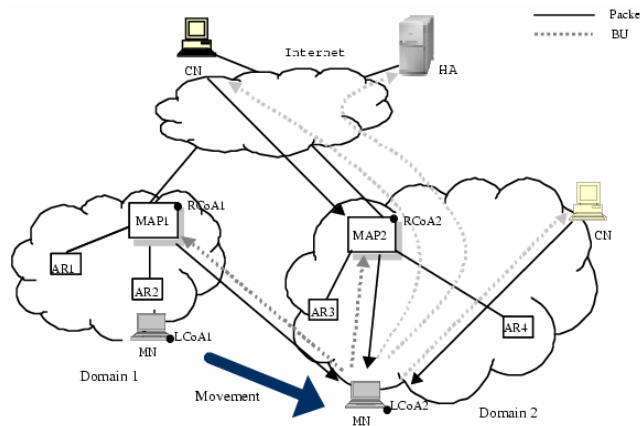


Fig. 1. Hierarchical mobile IPv6.

Let us consider the following situation: several kinds of people (e.g., office workers, housewives, shopkeepers, etc.) show comparatively regular movement patterns for some subnets; i.e., they will not move out for some time. In contrast, other kinds of people (e.g., taxi drivers, salesmen, etc.) move around quite randomly. If the information related to

each MN's past movements is maintained locally and is available, the proper BU lifetime can be given whenever the MN enters a subnet. In this work, three kinds of BU messages are used according to the lifetime:

- (1)  $BU_\alpha$  has a default lifetime ( $DLT$ ), which is used in MIPv6 [1]. After switching to a new MAP, the MN should send  $BU_\alpha$  to its HA and CNs, and may also send it to a previous MAP, asking it to redirect all incoming packets to the new CoA.
- (2)  $BU_\beta$  has an adaptive lifetime ( $LT_\beta$ ), which is computed based on the local profile. This value is the total time during which the current binding will be kept for the MN's home address. And, the number of  $Kbm$  is the result that this value is divided by 3.5 minutes [1]. The  $Kcredit$  value is calculated by using these values as stated in section 3.1.  $BU_\beta$  also includes  $Kcredit$  and has to be delivered to MAP, its HA and the CNs.
- (3)  $BU_0$  contains a zero lifetime value ( $LT_0$ ). When the MN moves into a subnet in another domain before  $BU_\alpha$  or  $BU_\beta$  expires, it will be used to notify both the HA and external CNs that the cached data for the current binding has become stale.

Only  $BU_\beta$  is newly proposed in this paper; the other two BUs were originally used in MIPv6. If the MN does not move out even when  $LT_\beta$  expires,  $BU_\alpha$  will be used thereafter. In the case of inter-domain movement, the MAP sends a  $BU_0$  to both HA and CNs to inform them that the current binding has become stale.

One thing to note here is that our approach does not incur an additional search cost although the MN leaves the current subnet before the lifetime expires. In MIPv6, movement detection is done through a router advertisement that contains a router advertisement interval [1], expressed in milliseconds. Thus, since movement detection in our schemes is the same as that in MIPv6, the router advertisement interval is small enough for the MN's movement to be detected.

### 3.3 Lifetime Calculation

Whenever an MN leaves a subnet, it records information (*a moving log*) about the visit. The log contains an ordered pair ( $l, AT, DT$ ), which includes a subnet identifier, the arrival time and the departure time. The average resident time per visited subnet is periodically calculated by using moving logs and is then recorded in the profile. This value will be used to compute the adaptive lifetime for  $BU_\beta$ . During this step, the number of logs per subnet is also considered since if the number of logs for a subnet is less than the threshold value ( $Count_b$ ), then we cannot get a reliable result. In the following subsections, two schemes will be proposed. The first considers only the average resident time for the current subnet. The second expands on the first by considering the visiting time region as well as the resident time.

#### 3.3.1 Resident time based scheme (RT)

First, the average resident time and the number of logs for each subnet are considered when the adaptive lifetime ( $LT_\beta$ ) is calculated. This scheme is called the *resident time based scheme (RT)*. When an MN moves from subnet  $m$  to another subnet, it records

a moving log for the current visit. Periodically, the average resident time for all visited subnets is calculated, and the algorithm for this purpose is shown in Fig. 2. The resident time ( $t_n$ ) for the  $n^{\text{th}}$  visit to subnet  $m$  is computed by subtracting the arrival time ( $AT$ ) from the departure time ( $DT$ ). As shown in Fig. 2, a comparison between  $t_n$  and  $\rho \times DLT$  is made to exclude the moving log when the resident time is small. Theoretically, it is reasonable that  $t_n$  should be compared with  $DLT$ . However, this will result in a great difference in performance since  $DLT$  is short (i.e.,  $DLT = 1$  second  $\sim 7$  minutes) [1]. Therefore, we assume that  $t_n$  is compared with  $\rho (\geq 1)$  times as long as  $DLT$ .  $Sum_m$  and  $Count_m$  are the total resident time and total number of visits to subnet  $m$ , respectively. In the calculation, if the number of visits to subnet  $m$  is less than a constant value ( $Count_b$ ), the  $BU_\alpha$  will be used, since poor (or no) regularity is found in subnet  $m$ .

```

// Whenever an MN moves out a subnet.
// Count_b: Threshold of Count
If (MN has visited subnet m) {
   $t_n = DT_n - AT_n$ 
  If ( $t_n > \rho \times DLT$ ) {
    Record moving log
     $Count_m = Count_m + 1$ 
     $Sum_m = Sum_m + t_n$ 
  }
}

// Periodic calculation
// LT: Lifetime
 $Mean_m = Sum_m / Count_m$ 
For (all moving logs to subnet m) {
  Calculate  $Var_m$  // Eq. (1)
  Determine mobility type
}
If ( $Count_m < Count_b$ )  $LT = DLT$ 
Else {
  If ( $Mean_m \leq \rho \times DLT$  or mobility type C)
     $LT = DLT$ 
  Else {
     $LT_\beta = Mean_m \times V$ 
     $LT = LT_\beta$ 
  }
}

```

Fig. 2. Resident time base scheme.

The calculated mean resident time can not be applied as is. It is just an average value, and there is no guarantee that the MN's next move will follow the profile. To deal this problem, we consider the variance rate,  $V$ , as well as the average resident time. To begin with, we classify the movement patterns for all subnets according to mobility types  $A$ ,  $B$  or  $C$  to show the degree of accuracy of the profile. In the case of mobility type  $A$ , the information in the profile is very trustworthy, while in the case of mobility type  $C$ , there is little (or no) regularity in the pattern in the current subnet. To quantify the difference, the variance is calculated for all subnets as shown in Eq. (1):

$$Var_m = \frac{1}{n} \sum_{i=1}^n (t_i - Mean_m)^2. \quad (1)$$

If  $Var_m$  is smaller than constant  $\delta_1$ , subnet  $m$  is classified as a mobility type  $A$  pattern. This means that if the MN visits the subnet again, it will reside there for approximately the mean resident time. If  $Var_m$  is larger than constant  $\delta_1$  and smaller than constant  $\delta_2$ , the subnet is classified as a mobility type  $B$  pattern. In this case, the MN will sometimes stay in the subnet much longer or shorter than the mean resident time. Otherwise, the subnet is classified as a mobility type  $C$  pattern, where the profile can not give reliable information. The lifetime value for the next BU is calculated by multiplying the mean resident time by the difference constant,  $V$ , according to its mobility type. This is, the constant value in mobility type  $A$  ( $V_A$ ) is larger than that in mobility type  $B$  ( $V_B$ ). The calculated value,  $LT_\beta$ , will be used as the lifetime for  $BU_\beta$  when the MN visits a subnet after creating the profile.

### 3.3.2 Time region based scheme (TR)

The resident time for some subnets often depends on the arrival time. Thus, we have devised another scheme called the *Time Region based scheme (TR)* by expanding *RT*. This scheme also uses the time region of the arrival time to enhance the accuracy of the profile. We observe that the MN visits the subnet frequently in the morning and afternoon (e.g., during office hours), but that the average resident time is not the same in both time regions. As a result, during periodic calculations, we have to consider the mean resident time per (subnet ID, time region) pair, not just the subnet. This means that there may be several mean resident times according to the time region in spite of the fact that the subnet remains the same. Thus, an algorithm to determine time regions from moving logs is needed. Five different cases are considered, as shown in Fig. 3. The following information is also maintained in the profile for each time region:

- $AT_{mn}^{high}$ : the highest (or latest) arrival time;
- $DT_{mn}^{low}$ : the lowest (or earliest) departure time;
- $Count_{mn}$ : the number of visits included in the  $n^{th}$  time region;
- $TotalCount_{mn}$ : the total number of visits considered in the  $n^{th}$  time region.

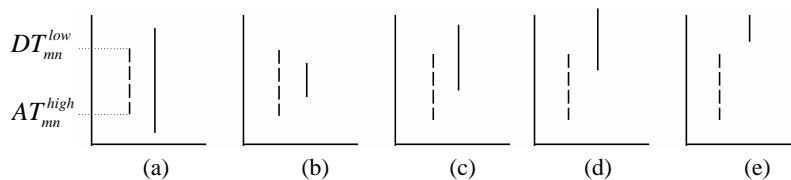


Fig. 3. Various visiting time cases.

Here, subscriptions  $n$  and  $m$  mean the  $n^{th}$  time region to subnet  $m$ . Since we consider the time region as well as the visiting subnet, each time region keeps a separate value for the number of visits ( $TotalCount_{mn}$ ,  $Count_{mn}$ ).

In Fig. 3, the dotted line represents the time interval ( $Interval_{mn} = DT_{mn}^{low} - AT_{mn}^{high}$ ) during which one time region is calculated. The solid line shows the current visiting time

(i.e. the time recorded in a moving log). In the case shown in Fig. 3 (e), it is natural to exclude a new visit from the time region. For the visit shown in Fig. 3 (a) or (b) we need to check whether the MN resides too long or not long enough in the subnet. If the resident time is longer than  $\frac{3}{2} \times Interval_{mn}$  or shorter than  $\frac{1}{2} \times Interval_{mn}$ , the difference between them will become too grate, and the current visiting log will not provide reliable information. Thus, the log is completely excluded; if not, the log is also used in periodic calculations. In addition, we must consider not only the resident time but also the time when an MN arrives. Figs. 3 (c) and (d) shows similar cases. However, if both cases are considered, the time region will not give useful information. Thus, the following process is needed to get an accurate determination:

---

middle =  $Interval_{mn}/2$   
 if (middle  $\geq$  the arrival time of the current visit)  
     include the current log in the  $n^{th}$  time region  
 else exclude the current log

---

Then, if the current log is included in  $n^{th}$  time region of subnet  $m$ ,  $Count_{mn}$  and  $TotalCount_{mn}$  both increase by 1; otherwise, only  $TotalCount_{mn}$  increases by 1 (See Figs. 3 (a) and (b)), since this variable will be used to determine the correctness of the profile. Of course, if the arrival time of the current visit is earlier than  $AT_{mn}^{high}$ , it is considered, contrary to the cases shown in Figs. 3 (c), (d) and (e). The moving log excluded from the above algorithm will be used to form another time region apart from the ones shown in Figs. 3 (a) and (b).

After time regions are determined in this way, the algorithm used to determine the mobility type is similar to  $RT$  with one difference. In  $RT$ , only  $Var_m$  is considered per visited subnet. However, both comparisons between the ratio  $Count_{mn}$  and  $TotalCount_{mn}$  and  $Var_m$  need to determine how useful the information about the time region is. That is, if  $Var_m$  is smaller than  $\delta_1$  and  $\frac{Count_{mn}}{TotalCount_{mn}}$  is larger than  $\gamma_1$ , then the time region to subnet  $m$  is regarded as a mobility type  $A$  pattern. If  $Var_m$  is greater than  $\delta_2$  or  $\frac{Count_{mn}}{TotalCount_{mn}}$  is smaller than  $\gamma_2$ , then it is concluded that there is no regularity (mobility type  $C$ ). In the other cases, the mean resident time is adjusted as mobility type  $B$ .

### 3.4 Disconnection

In our schemes, one of the main considerations is disconnection. If an MN cannot connect to its CNs or HA during communication, several packets will be lost. This is because the CNs think that the MN is alive and will continue getting packets until  $BU_\beta$  has expired. To cope with this situation, when an MN starts to send/receive packets, it is forced to send  $BU_\alpha$  first, which updates the binding cache in its HA and CNs. After communication ends, it checks whether  $LT_\beta$  in the MN has expired or not. If it has not, it calculates the remaining time ( $LT_{\beta new} = LT_\beta -$  the elapsed time during communication) and then sends a new  $BU_{\beta new}$ . Of course, if it has expired, the rest of the process is the same as that in HMIPv6 (see Fig. 4).

- When communication starts.
  - MN first sends  $BU_\alpha$
  - Packets are delivered
- When communication ends.
  - If ( $LT_\beta$  has not expired)
  - $LT_{\beta_{new}} = LT_\beta -$  (the elapse time during communication)
  - MN sends  $BU_{\beta_{new}}$
  - else
  - MN just sends  $BU_\alpha$

Fig. 4. The algorithm for disconnection.

While packets are being delivered,  $BU_\alpha$  is sent; thus, our schemes are not affected by inter- or intra-domain movement. It should be noted that the possibility of disconnection is generally very small because of the advanced mobile communications technology used, except in the case of voluntary power-off. In addition, it is expected that the MN will not be actively communicating most of the time [16]. Therefore, our schemes can work more efficiently than HMIPv6 even though disconnection occurs.

### 4. PERFORMANCE ANALYSIS

#### 4.1 Simulation Models

In this section, we will show the performance of our schemes based on simulation results. The simulation models for our schemes are briefly depicted in Fig. 5. Each MN collects log data that contain  $(l, AT_n, DT_n)$  whenever it leaves a visited subnet. In the case of  $TR$ , each MN gathers the same log data, but the main relevant information is the time region as well as the mean resident time.

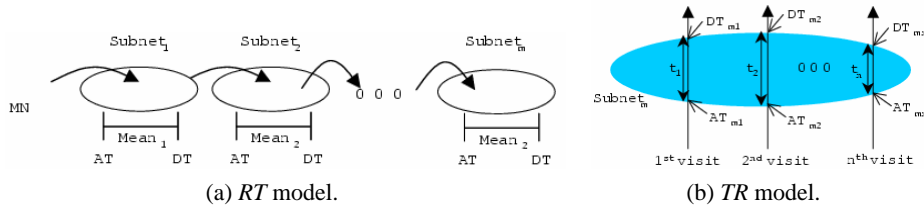


Fig. 5. Simulation models.

In the experiments, we assumed that the resident time at any subnet followed a Gamma distribution [17] with a shape parameter  $\alpha$ . Gamma distribution was selected because it can be shaped to represent various distributions as well as measured data that cannot be characterized by a particular distribution. Eqs. (2), (3) and (4) were used to calculate the density function, mean and variance, respectively, where  $t$  is the resident time at each visited subnet. The resident time followed an Exponential distribution, where parameters  $\alpha = 1$  and  $\lambda = 1/E(t)$  in the Gamma distribution. We conducted experiments to measure the number of BU messages from an MN based on Gamma and Exponential distributions.

$$f(t) = \frac{\lambda^\alpha}{\Gamma(\alpha)} (\lambda t)^{\alpha-1} e^{-\lambda t}, \quad t \geq 0, \quad (2)$$

$$E(t) = \frac{\alpha}{\lambda}, \quad (3)$$

$$V(t) = \frac{\alpha}{\lambda^2}. \quad (4)$$

However, the results will be shown based on the amount of bandwidth allocated by those messages. The disconnection rate ( $\zeta$ ) was set to 0.001, but this did not affect the overall performance.

The parameter settings, which were set as constants as described in the previous section, are shown in Table 1. Of course, the performance depended on these parameters. However, issues related to the degree of accuracy of the profile are beyond the scope of this paper.

**Table 1. Parameter settings.**

parameter	value	meaning
$\rho$	2	
$Count_b$	10	threshold of Count
$\delta_1$	10	constant value to determine mobility type A
$\delta_2$	50	constant value to determine mobility type C
$\gamma_1$	0.8	constant value of $\frac{Count_{mn}}{TotalCount_{mn}}$ for mobility type A
$\gamma_2$	0.6	constant value of $\frac{Count_{mn}}{TotalCount_{mn}}$ for mobility type C
$\kappa$	0.3	intra-domain moving rate
$V_A$	1.0	V value for mobility type A
$V_B$	0.8	V value for mobility type B
$\zeta$	0.001	disconnection rate

## 4.2 The Results

In the experiments, our main aim was to compare our schemes with MIP by considering the allocated bandwidth for BU messages. To do so, we tried to evaluate the aggregated signaling bandwidth consumed on the Internet. First, we assumed that there were no errors in message delivery. Before explaining our results, we should point out that  $DLT$  is a very small value (i.e.,  $DLT = 1$  seconds  $\sim$  7 minutes) [1]. On the other hand, any regular movement pattern found in the profile means that the MN may stay for a period of time that is considerably longer than  $DLT$  (i.e., perhaps more than several minutes). Intuitively, our schemes would show better performance than MIP. Therefore,  $DLT$  was set to 7 minutes in the experiments as a maximum value in MIP. Thus, instead of a simple comparison between the numbers of BU messages, we will show the performance improvement in terms of the BU bandwidth usage of our scheme compared with that of MIP. The three bandwidths were defined as follows:

$$BW_{MIPv6} = Size_{BU} \times \{ \kappa \times (f_{CN} \times (\#CN + 1) + f_{HA}) + (1 - \kappa) \times (M \times \#CN + 2) \}, \quad (5)$$

$$BW_{HMIPv6} = Size_{BU} \times \{ \kappa \times (f_{REF} \times (\#CN + 1) + (1 - \kappa) \times (M \times \#CN + 2)) \}, \quad (6)$$

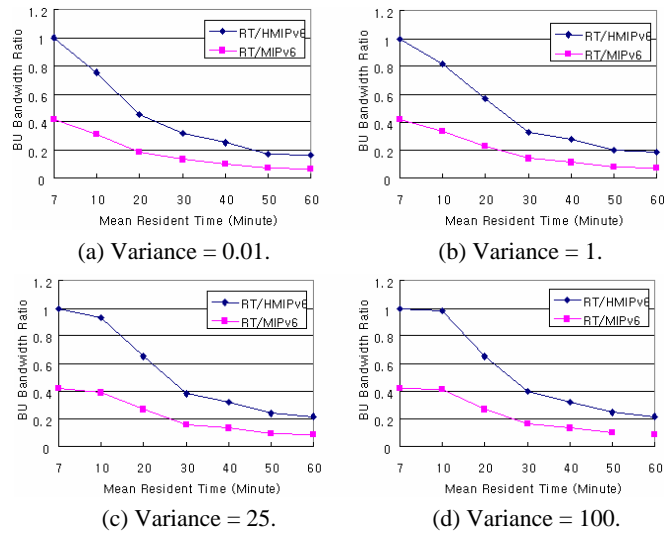
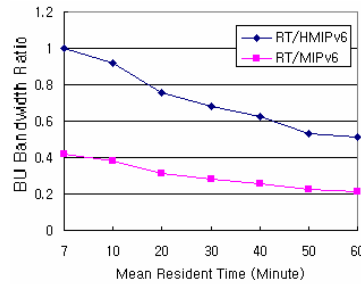
$$BW_{proposal} = Size_{BU} \times \{ \kappa \times (f_{RT-REF} \times (\#CN + 1) + (1 - \kappa) \times (M \times \#CN + 2) + f_{ADD}) \}, \quad (7)$$

$$f_{ADD} = \begin{cases} \#CN + 1, & \text{if the visiting subnet is in the profile} \\ 0, & \text{otherwise} \end{cases},$$

where  $Size_{BU}$  is the size of a BU (68bytes = IPv6 header (40bytes) + Binding Update Extension Header (28bytes)) [18].  $f_{HA}$  denotes the BU emission frequency from the MN to its HA, and  $f_{CN}$  denotes the average BU emission frequency from the MN to its CNs. When an MN moves,  $\kappa$  represents the intra-domain moving rate. The domain-crossing rate is  $1 - \kappa$ , which is the number of crossing domains divided by the total number of crossing subnets. The MN sends  $M$  consecutive BUs to its external CNs, sends another BU to its HA and receives one BA from HA. In Eq. (5) [18],  $\#CN$  represents the number of CNs that are not in the home network. When an MN, using MIPv6, is moving among subnets, it sends a BU to each CN and to its HA, equal to  $f_{CN}$  and  $f_{HA}$ . In Eq. (6) [18],  $\#CN$  represents the number of external CNs of the MN. When it is moving within a foreign domain in HMIPv6, a BU is also sent to both the external CNs and HA at a refreshment frequency equal to  $f_{REF}$ . If it can utilize the information in the local profile as proposed in this paper, the refreshment frequency can be reduced to  $f_{RT-REF}$  although the MAP should send an additional BU,  $f_{ADD}$ , to its external CNs and HA (Eq. (7)). However, as this is the inter-domain movement, the total amount of the bandwidth allocated to BUs is the same in all three schemes.

Fig. 6 shows a comparison between  $RT$  and MIP in terms of the Gamma distribution, where the variance was set to 0.01, 1, 25 and 100, and the mean resident time varied from 7 to 60 minutes. The results shown in Fig. 7 were obtained with an Exponential distribution. We assumed that an MN moved around according to mobility type  $A$  among 15% of the subnets recorded in the profile, according to mobility type  $B$  in another 30% of the subnets, and according to mobility type  $C$  in the remaining 55%. During local movement within a foreign domain, the BU bandwidth depended on  $\#CN$ ,  $f_{CN}$ ,  $f_{HA}$ ,  $f_{REF}$ , and  $f_{RT-REF}$ . Since the behavior of the BU bandwidth ratio are almost the same whether  $\#CN$  was 2 or 10, we display only four results in Fig. 6 for the case in which  $\#CN$  was two.

The variance and the function of the resident time distribution rarely influenced the overall performance, as shown in Figs. 6 and 7. On the whole, from these figures, we find that  $RT$  over MIPv6 achieves better bandwidth usage than  $RT$  over HMIPv6. The reason is that in the case of MIPv6, BUs are sent to the HA and CNs when the MN is roaming locally, but HMIPv6 sends refresh BUs to the MAP periodically. Both the ratio of  $RT$  to MIPv6 and the ratio of  $RT$  to HMIPv6 decrease as the mean resident time increases. If a long mean resident time was determined from the profile and applied to the lifetime, the lifetime for the next BU was set to be a large value. Of course, there could be a great difference between mean and real resident times due to different mobility types. Despite this fact, the amount of saved bandwidth was very great in some subnets when they were determined to be either mobility type  $A$  or  $B$ . In particular, when an MN

Fig. 6. The effect of the Gamma distribution in  $RT$ .Fig. 7. The effect of the exponential distribution in  $RT$ .

moved into another domain frequently, most of the signaling load was generated by the refreshment BUs. Our main improvement was achieved by decreasing the number of periodic refreshment BUs. If an MN moved from the current subnet before the lifetime expired, an additional  $f_{ADD}$  had to be delivered. It was problematic since an MN would not follow the previous movement pattern, especially when the current resident time was shorter than the determined lifetime. However, if the current resident time was longer than 7 minutes, the number of BU messages could be greatly reduced. The results also show that the mean resident time may be much longer than 60 minutes in reality, although the time varied from 7 to 60 minutes in the experiments. Thus, the energy efficiency of our schemes can be improved more than the results obtained in this study indicate. Of course, if an algorithm used to extract useful and reliable information from the profile is devised, the efficiency can be improved even more.

The second experiment examined the effects on the time region in the arrival time. The ratio of  $TR$  to  $RT$  was determined under Gamma and Exponential distributions. In the experiments, we only considered subnets where good regularity could be obtained

from the profile. It was assumed that 40% of the subnets recorded as mobility type *A* or *B* in the profile had only one time region, that another 40% of the subnets had two time regions, and that the remaining subnets had three time regions.

As shown in Fig. 8, the ratio of *TR* to *RT* under both distributions was not the same, but the difference was not great and decreased quickly as the mean resident time increased from 10 to 30 minutes. This indicates that if an MN regularly resides in a subnet for more than 30 minutes, the information from the profile may be very useful. Of course, experimental environments may be set up differently, so this value of 30 minutes may change. However, if we know the value, it will be very useful for enhancing the accuracy of the profile information. From the figure, *TR* also shows improved bandwidth usage compared to *RT* for most of the mean resident times. The reason can be found in the information in the profile. If there are two or more time regions in subnet *m* and if the mean resident times are not the same, then  $Var_m$  also will have a high value, which will determine whether the subnet is mobility B or C in *RT*. On the other hand, *TR* can diminish  $Var_m$  by grouping the logs into time regions.

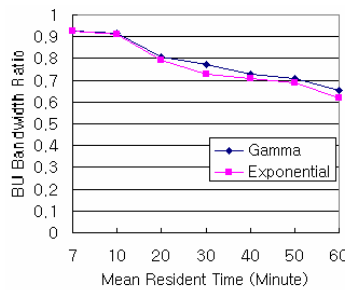


Fig. 8. The comparison of *RT* and *TR* in Gamma and Exponential distribution.

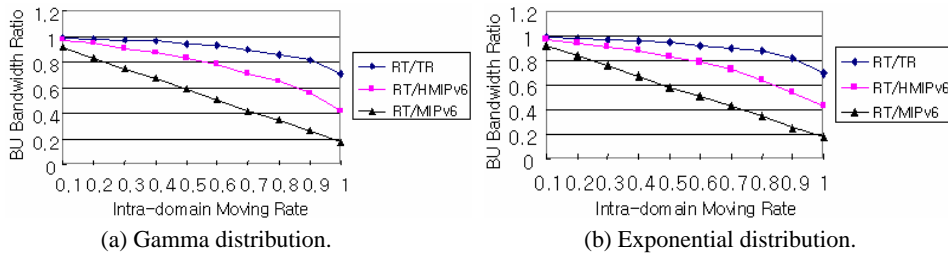


Fig. 9. The comparison of BU bandwidth various intra-domain moving ratio.

Fig. 9 shows the effect of the intra-domain moving rate ( $\kappa$ ) when an MN is roaming locally within a domain. As  $\kappa$  increases, the number of BUs sent to its HA and CNs increases in MIPv6. HMIPv6 avoids the transmission of such BUs and only sends a BU to the MAP, so the BU bandwidth becomes smaller than that of MIPv6. Furthermore, *RT* reduces the transmission frequency,  $f_{REF}$ , in HMIPv6 to  $f_{RT-REF}$ ; consequently, the bandwidth is used more efficiently. Meanwhile, as  $\kappa$  increases, the BU bandwidth in *TR* in-

creases more than it does in *RT*. The reason is that the detailed information in the profile is applied to *TR* within the MAP domain. In other words, the number of BUs sent to the HA and CNs becomes larger than that with *RT* when the MN is moving within the MAP. However, its HA and CNs maintain a more correct binding cache in *TR* than in *RT*.

## 5. CONCLUSION

In this paper, we have proposed lifetime determination schemes (*TR* and *RT*) for BUs in HMIPv6. By capturing some regularity in the movement patterns of MNs, we can reduce the overhead incurred by numerous BUs. From an MN's arrival time as well as the resident time at visited subnets, the lifetime can be determined dynamically. A process for evaluating the reliability of the information in the profile has also been devised. The main contribution of our schemes is that they reduce the number of BU messages and, thus, improve the energy efficiency.

Since our schemes are based on local profiles, a technique to enhance the accuracy of the calculated information is needed. That is, we still need to study further the accuracy of the profile and determine the effects of each parameter through the use of data mining algorithms.

## REFERENCES

1. D. B. Johnson, C. Perkins, and J. Arkko, "Mobility support in IPv6," RFC 3775, 2004.
2. A. Patel, K. Leung, H. Akhtar, M. Khalil, and K. Chowdhury, "Authentication protocol for mobile IPv6," *IETF Internet Draft*, draft-patel-mipv6-auth-protocol-00.txt, 2004.
3. J. Arkko and C. Vogt, "Credit-based authorization for binding lifetime extension," draft-arkko-mipv6-binding-lifetime-extension-00, 2004.
4. S. Tabbance, "Modeling the MSC/VLR processing load due to mobility management," in *Proceedings of the IEEE International Conference on Universal Personal Communications*, Vol. 1, 1998, pp. 741-744.
5. G. P. Pollini and C. L. I, "A profile-based location strategy and its performance," *IEEE Selected Areas in Communications*, Vol. 15, 1997, pp. 1415-1424.
6. H. K. Wu, M. H. Jin, J. T. Horng, and C. Y. Ke, "Personal paging area based on mobile's moving behaviors," in *Proceedings of the IEEE Computer and Communications Societies*, Vol. 1, 2001, pp. 21-35.
7. J. S. M. Ho and J. Xu, "History-based location tracking for personal communications networks," in *Proceedings of 48th IEEE Vehicular Technology Conference*, Vol. 1, 1998, pp. 244-248.
8. N. Adly and A. El-Nahas, "A profile-based hierarchical location management scheme for future PCS," in *Proceedings of 11th International Workshop on Database and Expert Systems Applications*, 2000, pp. 204-208.
9. T. Yang, Y. Dong, B. Zhou, and D. Makrakis, "Profile-based mobile MPLS protocol," in *Proceedings of the IEEE Canadian Conference on Electrical and Computer Engineering*, Vol. 3, 2002, pp. 1352-1356.

10. K. Wu, J. Harms, and E. S. Elmallah, "Profile-based protocols in wireless mobile ad hoc networks," in *Proceedings of 26th Annual IEEE Conference on Local Computer Networks*, 2001, pp. 568-575.
11. T. Kumagai, T. Asaka, and T. Takahashi, "Location management using mobile history for hierarchical mobile IPv6 networks," *IEICE Transaction on Communication*, Vol. E67-B, 2004, pp. 2567-2575.
12. Y. H. Han, J. M. Gil, and C. S. Hwang, "Route optimization by the use of two care-of addresses in hierarchical MIPv6," *IEICE Transaction on Communication*, Vol. E84-B, 2001, pp. 892-902.
13. T. Aura and J. Arkko, "MIPv6 BU attacks and defenses," *IETF Internet Draft draft-aura-mipv6-bu-attacks-01.txt*, Feb. 2002.
14. W. Haddad, L. Madour, J. Arkko, and F. Dupont, "Applying cryptographically generated addresses to OMIPv6 (OMIPv6+)," draft-haddad-Mmipv6-cga-omipv6-00 (work in progress), 2004.
15. H. Soliman, C. Castellucia, K. E. Malki, and L. Bellier, "Hierarchical MIPv6 mobility management (HMIPv6)," *IETF Internet Draft*, draft-ietf-mobileip-hmipv6-08.txt, 2003.
16. X. Zhang, J. G. Castellanos, and A. T. Campell, "P-MIP: paging extensions for mobile IP," *Mobile Networks and Applications*, Vol. 7, 2002, pp. 127-141.
17. Y. B. Lin, W. R. Lai, and R. J. Chen, "Performance analysis for dual band PCS networks," *IEEE Journal on Transactions on Computers*, Vol. 49, 2000, pp. 148-159.
18. C. Castelluccia, "HMIPv6: A hierarchical mobile IPv6 proposal," *ACM SIGMOBILE Mobile Computing and Communications Review (MC2R)*, Vol. 4, 2000, pp. 48-59.



**Sun Ok Yang (梁順玉)** received her M.S. and Ph.D. degrees in Computer Science and Engineering from Korea University, Seoul, South Korea in 2002 and 2006, respectively. Also, she is currently a Researcher in the Institute of Computer Science Technology at Korea University. Her research interests include mobility management and QoS provision issues in the next-generation wireless/mobile/sensor networks.



**SungSuk Kim (金星錫)** received the Ph.D. degree in Computer Science and Engineering from Korea University, Seoul, South Korea, in 2003. Currently, he is an Assistant Professor in the Department of Electronic Business at Seokyeong University. His primary research interests lie in the areas of mobile/pervasive computing, data management, and spatial databases. He is a member of the ACM.



**Chong-Sun Hwang (黃鍾善)** received his B.S. and M.S. degrees in Mathematics from Korea University, Seoul, South Korea, in 1966 and 1970, respectively. He received his Ph.D. in Computer Science and Statistics from University of Georgia in 1978. He is currently a professor in Dept. of Computer Science and Engineering, Korea University, Seoul, South Korea. His research interests include mobile computing systems, parallel and distributed database systems, and knowledge-based systems.